Unsteady Computation of Over-Expanded Flow in a Convergent Divergent Nozzle

Rahul B.V[1], Swapneel Roy[2], Thanusha M.T[3], and A.A.Khan[4]

Propulsion Division, National Aerospace Laboratories, Bangalore
(COUNCIL OF SCIENTIFIC AND INDUSTRIAL RESEARCH, INDIA)

[1, 2, 3] Student Member, Aeronautical Society of India, 13B, Indraprastha Estate, New Delhi
[4] Scientist, Propulsion Division, National Aerospace Laboratories, Belur, Bangalore-560037
Email: ashfaque@nal.res.in, Phone: +91-80-25051605,
Fax: +91-80-25222494

Abstracts

The classical one-dimensional inviscid theory does not reveal the complex flow features in an over-expanded nozzle accurately. The code Fluent has been used to simulate the transient flow passing through a 2-D Convergent-Divergent (CD) nozzle (A_e/A_t=1.7, α_e=3.03^0, Symmetric about centerline) for nozzle pressure ratios (NPR) corresponding to over-expanded flow. The transient RANS equation with Shear Stress Transport k-ω (SSTKW) turbulence model has been simulated. Both inviscid and viscous flows have been simulated. Both the first order and second order upwind scheme has been used for all the conservation equations. The inviscid solutions predicted steady results for both first and second order simulations after a certain time. There is no significant unsteadiness in the first order viscous solutions too. Shock structure is also symmetric in the first order viscous predictions for all NPRs. However, second order viscous predictions captured unsteadiness, lambda shock, aftershock and flow separation (FSS and RSS) depending upon NPRs. The lambda shock becomes asymmetric after a certain time for NPR≥1.41. The flow unsteadiness is significant with asymmetric lambda shock. The shock oscillates with the asymmetry. The number of aftershock increases and the size of Mach stem reduces with increase in NPR. The computed solutions differ from the simple theory as far as shock location, shock structure, normal shock strength and aftershocks are concerned. However, the 2nd order viscous predicted results (shock structure, shock location, size of normal shock, aftershock, and asymmetric lambda shocks) are close to the experiments in most of the cases.

Nomenclature

A = Nozzle area

M = Local Mach number

P, P_0 = Static, Total pressure

T, T_0 = Static, Total temperature

V= Velocity

α = Half nozzle wall angle

Cp = Specific heat at constant pressure

Δx, Δt = grid size, Time step respectively

Subscript

t, e, s = throat, exit, shock respectively

Acronym

NPR = Nozzle Pressure Ratio (P_0/P_e)

FSS = Free Shock Separation

RSS = Restricted Shock Separation

1. INTRODUCTION

The one-dimensional inviscid isentropic flow in a CD nozzle is a classical text-book problem, which has different flow regimes depending upon NPR. The inviscid theory predicts a simple shock structure consisting of a normal shock followed by a smooth recovery to exit pressure in the divergence part of a choked nozzle for NPRs corresponding to the over-expanded flow regime. But, in reality, multi-dimensionality and viscous effects like wall boundary layer and flow separation drastically alter the flow in a CD nozzle. Stable separation (with a passive porous cavity) could improve the thrust efficiency of off-design Nozzle [1]. Viscous effects thicken the boundary layer before the shock and the base of the shock also becomes thick or bifurcate the shock in the form of lambda shape depending upon the nature and thickness of boundary layer [2]. So, the shock contains normal shock known as Mach stem in the central region while the shocks close to both the boundaries become thicker or bifurcate as lambda shock. The first leg of the lambda shock (known as incident shock) turns the flow away from the wall while the second leg (known as reflected shock) tries to turn back the flow to the original direction. The coincidence of Mach stem, incident shock and reflected shock is known as triple point. At higher NPR, the flow separation in CD Nozzle is asymmetric, where one lambda foot is larger than the other. The asymmetric flow separation has been predicted for higher NPR (1.5<NPR<2.4) depending upon the initial flow field [3]. The whole flow behind the lambda shock is divided into two region separated by slip stream. The slip stream originates from the triple point [4-5]. The flow behind the Mach stem (away from the boundary) becomes subsonic because of the normal shock in the central region. However, the flow behind the reflected shock is still supersonic. Since the area between the slip stream and shear layer behind the reflected shock is increasing for a short distance, hence, the flow accelerates for a certain distance with expansion wave. The central region of the flow becomes subsonic behind the Mach stem. But it also

ISBN : 978-81-921580-8-2

accelerates because of convergent-divergent region made by wavy slip stream. The slip stream becomes supersonic at the position where it is intercepted by the expansion wave [5]. Ultimately, the flow may experience another shock in the downstream known as aftershock to match the ambient pressure. For higher NPR (NPR≥2), the separation is not the result of a stronger shock/boundary layer interaction, but it comes through the natural tendency of an over-expanded nozzle flow [6-7].

Two different patterns of flow separation may occur in over-expanded nozzle (Free shock separation and Restricted shock separation). In free shock separation (FSS), the flow separates from the wall and separation continues till the exit of the nozzle. However, in restricted shock separation (RSS), the separated flow reattaches to the wall and becomes supersonic in the downstream of the reattachment point [8-11]. The peak value of wall static pressure is associated with reattachment of flow [12].

Two different vortical regions have been found during nozzle start up [13]. One vortex is due to the boundary layer separation from wall, whereas the second vortex spreads in the divergent section and has inviscid origin. The unsteady nature of shock boundary interaction is explained in [14-15]. The over-expanded nozzles are characterized by unsteady shock induced separation.

The CFL criterion for stability should be ≤ 1. The CFL relation is given by

$$\frac{V \times \Delta t}{\Delta x} \leq 1$$

The over-expanded flow regime in CD nozzles of different shapes and sizes has been a subject matter of numerous investigations because of their wide range of applications. The asymmetry in the lambda shock is a key factor for mixing enhancement [16]. Investigation [16] contains detailed experimental study of flow in rectangular over-expanded supersonic nozzles exploring the complex nature of such flows. The prediction of such flows also presents a great challenge to any CFD code. The present computational work was aimed at simulating transient flow in one CD nozzle of Reference [16] for the given range of NPRs with the help of a commercial CFD code Fluent, with the objective of understanding the complex flow structure in a CD nozzle.

2. COMPUTATIONAL DETAILS

The computational domain for the CD nozzle has been generated based on the information given in the reference [16]. GAMBIT has been used to generate geometry and grid in the computational domain. The code Fluent has been used to solve 2-D transient Reynolds-averaged Navier-Stokes (RANS) equations in the CD nozzle (A_e/A_t=1.7, α_e=3.03^0, symmetric about centerline) for different NPRs. Both first and second order upwind scheme have been used for all the conservation equations for inviscid and viscous simulations. The second order inviscid simulations have been made after getting convergence with first order schemes. However, viscous flows have been simulated with second order upwind schemes twice (1. initialized with inlet conditions, 2. initialized with first order converged solutions). Boundary layer grid has been generated to capture the boundary layer effect. Based on the previous experience, SSTKW turbulence model has been chosen for the simulation. The inlet boundary conditions consisted of total pressure, P_0=3.5x10^5 N/m^2 and total temperature, T_0=300K. The exit static pressure was varied to obtain different NPRs (NPR=1.20, 1.25, 1.32, 1.41, 1.65, 1.92, 2.03 and 2.36). For stability of the unsteady simulation, the time step Δt has been taken as 2.0 e-06 based on the CFL criterion. The grid size for the flow domain is 143 x 41.

3. RESULTS AND DISCUSSION

Unsteadiness has not been found in the inviscid predictions for all NPRs. In addition, the predicted inviscid solutions are close to 1-D inviscid theory in regard of shock location and shock structure (one normal shock followed by smooth recovery of pressure) for lower NPRs. For higher NPRs, the theoretical area ratio (A_e/A_t) at the shock location is higher than the exit area ratio (i.e. Shock location is outside the Nozzle). But, inviscid solution predicted shock at the exit itself for higher NPRs to match static pressure specified at the outlet boundary condition. The locations of shock for inviscid predictions are compared with the theoretical values in Table1. The second order predictions are better than the first order as shown in Table1.

The flow becomes steady after a certain time (approximately 4-5ms) in case of viscous prediction with 1st order upwind discretization. The 1st order viscous solution is different from the inviscid solutions in regard of shock structure and shock location. Symmetric lambda shock near the wall, Mach stem in the central region and flow separation downstream of the shock have been observed for NPR≥1.32 in 1st order viscous predictions. However, the 2nd order upwind discretized solutions looked to be transient in nature even after 10ms for NPR≥1.41. The converged solutions predicted lambda shock near the wall, Mach stem in the central region, flow separation and after shock in the divergent part of the nozzle. The lambda shock is symmetric for lower NPRs. However, it becomes asymmetric for NPR≥1.41. Boundary layer shock interaction converts the normal shock into two oblique shocks (incident and reflected shock) in boundary layer region. The flow compresses through the incident shock and turn the flow away from the wall. Because of the turning of flow towards the center, the flow separates and the effective area of the flow reduces from the geometric area. The reflected shock tries to turn the flow towards original flow direction. The flow behind the reflected shock is still supersonic for a small region just above the shear layer. The whole flow behind the lambda shock is divided into two region separated by slip stream as shown in Fig. 1 schematically. The sonic line disappears after short distance from the main shock which indicates that the slip line becomes supersonic. This supersonic flow again experiences a shock depending upon the exit pressure. This shock is known as aftershock. The separated flow is reattached (RSS) for lower NPRs. However, it becomes FSS at the larger leg of the

ISBN : 978-81-921580-8-2

lambda shock for NPR≥1.92. The location of shock is significantly different from the inviscid theory. However, the viscous predictions are close to the experimental values as shown in Table 2. The 1st order solutions could not capture the aftershock as shown in Fig. 2 (Mach number plot at the Mach stem for different NPRs – 1st order upwind prediction). However, the 2nd order solutions predicted one aftershock for NPR=1.41, two aftershocks for NPR=1.65 and three aftershocks for NPR=1.92 as shown in Fig. 3 (Mach number plot at Mach stem for different NPRs – 2nd order upwind prediction). The number of aftershocks increases with increase in NPR. Atleast one aftershock for NPR≥1.41 and atleast two aftershocks for NPR≥1.92 have been observed in the experiments too. The 2nd order solutions also predicted lambda shock for NPR≥1.25. The shock structure is symmetric for the whole simulation time (20ms) for NPR≤1.32. However, it converts to an asymmetric lambda shock [i.e. one side (e.g. top wall) of the lambda shock is larger than the other side (e.g. bottom wall)] after a certain time (5-15ms) for higher NPRs (NPR≥1.41). It is very difficult to justify the asymmetry in lambda shock in a simulation where geometry and boundary conditions are symmetric and uniform respectively. But it could be coanda effect. The experimental results also indicate the symmetric shock structure for NPR≤1.32 and asymmetric lambda shock for NPR≥1.41. Fig. 4 shows predicted Mach number contours of the nozzle at two different times (4ms and 12ms) for NPR=1.92. It clearly shows the conversion of symmetric lambda shock to asymmetric lambda shock after a certain time. This time reduces with increase in NPR. The pattern of asymmetry has been found to be different in different NPRs. Larger leg of the lambda shock may be either side (i.e. top wall or bottom wall). But the asymmetry does not flip within a simulation. The lambda shock has been found to be oscillating after the conversion to asymmetry. The size of Mach stem reduces with increase in NPR. The location of shock shifted towards upstream with viscous prediction. The 2nd order solutions further shifts it upstream for NPR≥1.32. Also, the shock location has been found to shift towards upstream with the conversion to asymmetric lambda shock. Fig. 5 and Fig. 6 show the plots of wall shear stress and wall pressure of the nozzle at the same times (4ms and 12ms), as shown in Fig. 4, for NPR=1.92 respectively. Fig. 5 clearly indicates the significant reduction in wall shear stress with the shock and then increase in the wall shear stress behind the shock at both the walls. In addition, wall shear stress on both the walls coincide each other in case of symmetric lambda shock (Fig.5a). It also indicates the negative value of wall shear stress throughout behind the shock in case of symmetric lambda shock (Fig. 5a). This is the case of FSS at both the walls. However, asymmetric lambda shock changes the wall shear stress distribution (Fig. 5b). The wall shear stress is no more coincident behind the shock. At the top wall, where the lambda shock contains smaller legs, the wall shear stress becomes positive behind shock after a certain distance in the downstream. This indicates the reattachment of the separated flow at the top wall. This is the case of RSS at the top wall. However, the bottom wall, where the lambda shock contains larger leg, shows negative value of wall shear stress behind the shock (FSS) in case of asymmetric shock pattern too. Fig. 6 shows similar pattern for wall pressure as shown in Fig. 5 for wall shear stress. Fig. 6 indicates the increase in wall pressure behind the shock. Fig. 6a also indicates the coincidence of wall pressure on the top and bottom wall in case of symmetric lambda shock. However, asymmetric lambda shock changes the wall pressure distribution. The wall pressure is not coincident on both the walls (Fig 6b). The free shock separated wall (bottom wall) shows slightly higher wall pressure in the separated flow region as compared to the restricted shock separated wall. However, it becomes opposite after the reattachment of flow at the restricted shock separated wall (top wall) for a certain distance in the downstream. In the downstream, the top wall shows more oscillation in the wall pressure as compared to that of bottom wall. Fig. 7 shows Mach number contours of four different NPRs at flow time ≥ 20ms. It clearly shows the shock patterns (symmetric lambda shock at lower NPR, asymmetric lambda shock at higher NPRs, aftershock(s) at higher NPRs) at different NPRs as mentioned in this paper.

4. CONCLUSION

The flow in a CD nozzle in over-expanded flow regime is quite complex. The one-dimensional inviscid theory cannot reveal all the flow features correctly. One can capture such complex flows by employing a CFD code. The code Fluent has been successfully used here to compute the real life flow features like symmetric and asymmetric lambda shock depending upon NPR, location of shock and aftershocks in a CD nozzle. The major conclusions of this study are as follows

A. *Flow unsteadiness:*

There is no unsteady in flow for inviscid flow predictions. The first order viscous solutions also do not show any significant unsteadiness in the flow. The flow becomes unsteady in nature in cases where lambda shock becomes asymmetric and wall pressure and wall shear stress at top and bottom wall do not coincide.

B. *Shock Location:*

There is a significant variation in shock location between viscous and inviscid solutions. The inviscid prediction of shock location in the form of area ratio agrees well with the corresponding theoretical values for those NPRs where shock is located in the divergent section of the Nozzle. However, viscous flow shifts the shock towards upstream. The viscous prediction of shock location is generally close to the experiments [16].

C. *Shock structure (Lambda shock and aftershock):*

The 1st order viscous predictions captured symmetric lambda shock which cannot be explained with one-dimensional inviscid theory. However, asymmetric lambda shock and aftershock for higher NPRs could not be captured in 1st order viscous predictions. The 2nd order viscous solutions predicted lambda shocks for NPR≥1.32, symmetric lambda shocks for NPR=1.32, asymmetric lambda shocks for

ISBN : 978-81-921580-8-2

NPR≥1.41, one aftershock for NPR=1.41, two aftershocks for NPR=1.65 and three aftershocks for NPR=1.92, which cannot be explained with one dimensional inviscid theory. The different kind of lambda shocks (symmetric, asymmetric) and different number of aftershocks depending upon NPRs have been observed in the experiments too [16].

D. *Flow Separation:*

The separation of flow has been predicted in viscous computations. Generally, for nozzle flow with asymmetric lambda shock, the smaller leg side of lambda shock reattaches behind the shock after a certain distance (RSS). However, the larger leg side of the lambda shock continues to be separated till the exit of the nozzle without reattachment (FSS).

5. FIGURES & TABLES

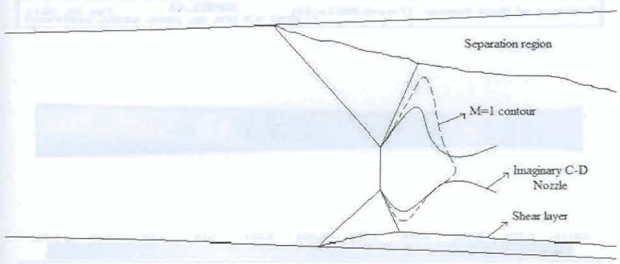

Fig. 1– Equivalent C-D Nozzle in Mach stem region

Table 1 – Comparison of shock locations for Inviscid flow analysis

NPR	Shock Location (in A_s/A_t)		
	1storder	2ndorder	Theoretical
1.2	1.109	1.153	1.176
1.25	1.153	1.216	1.234
1.32	1.234	1.284	1.3145
1.41	1.326	1.377	1.407
1.65	1.537	1.598	1.64
1.92	1.592	1.65	1.823
2.03	1.605	1.658	1.885
2.36	1.623	1.658	2.032

Table 2 – Comparison of shock locations for Viscous flow analysis

NPR	Shock Location (in A_s/A_t)			
	1storder	2ndorder	Experimental	Theoretical (Inviscid)
1.2	1.04	1.064	1.04	1.176
1.25	1.076	1.093	1.09	1.234
1.32	1.127	1.126	1.14	1.3145
1.41	1.175	1.14	1.18	1.407
1.65	1.291	1.215	1.31	1.64
1.92	1.391	1.292	1.38	1.823
2.03	1.426	1.334	1.38	1.885
2.36	1.516	1.425	1.49	2.032

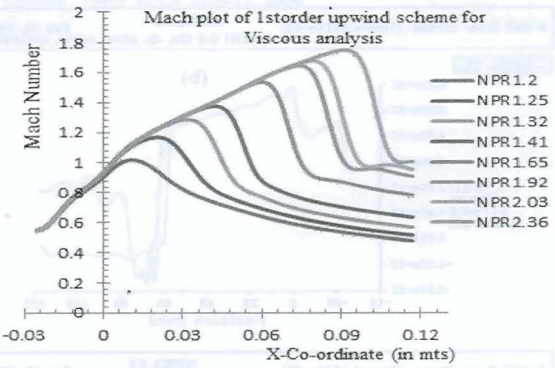

Fig. 2- Mach number plot at the centerline for 1st order viscous analysis

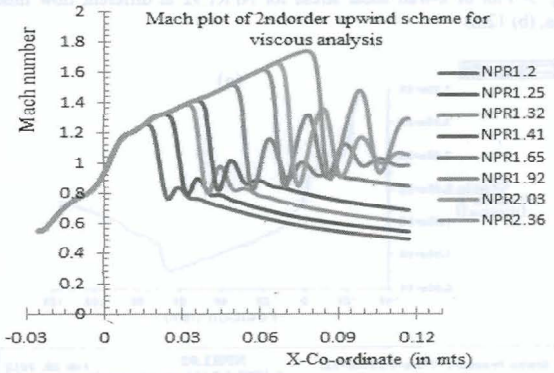

Fig. 3- Mach number plot at Mach stem for 2nd order viscous analysis

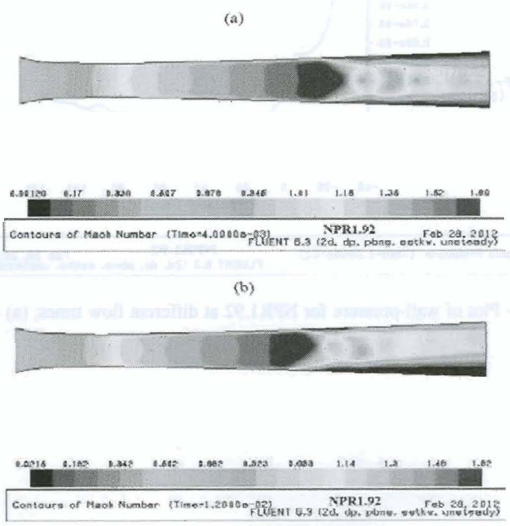

Fig. 4- Mach number contour for NPR1.92 at different flow times; (a) 4ms, (b) 12ms

ISBN : 978-81-921580-8-2

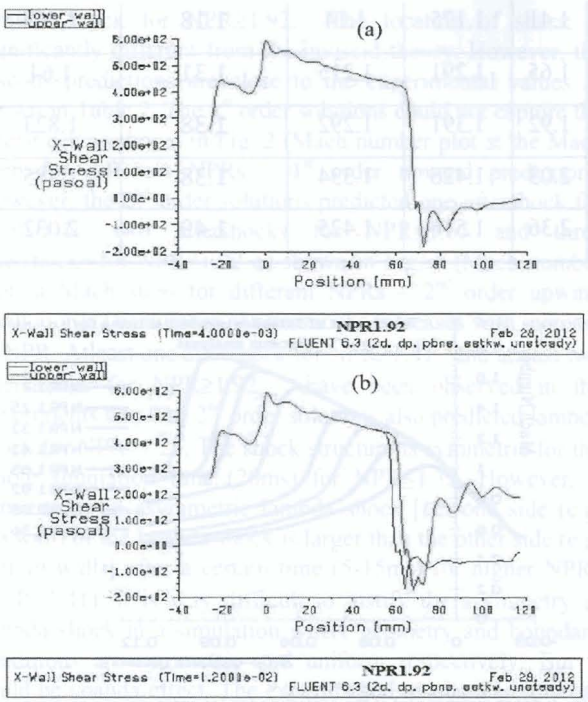

Fig. 5- Plot of x-wall shear stress for NPR1.92 at different flow times; (a) 4ms, (b) 12ms

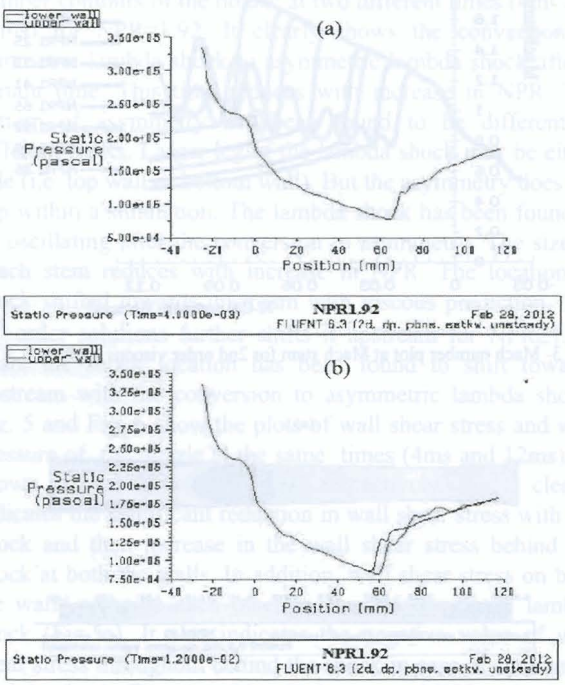

Fig. 6- Plot of wall-pressure for NPR1.92 at different flow times; (a) 4ms, (b) 12ms

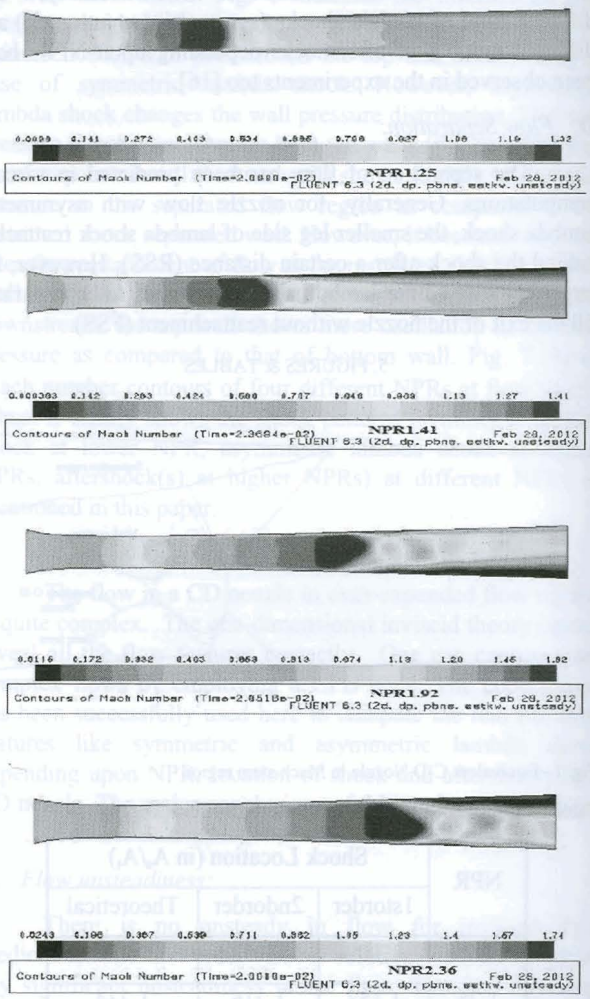

Fig. 7- Mach number contour for different NPRs

6. ACKNOWLEDGEMENT

The authors would like to thank the CSIR center C-MMACS, Bangalore for providing their computing facilities for this work.

REFERENCES

1. Scott C. Asbury, Christopher L. Gunther and Craig A. Hunter, "A passive Cavity Concept for Improving the Off-Design Performance of Fixed-Geometry Exhaust Nozzles" Paper AIAA 1996-2541, 1996

2. A. A. Khan and T. R. Shembharkar, "Viscous Flow Analysis in a Convergent-Divergent Nozzle" Proceedings of International Conference on Aerospace Science and Technology, INCAST 2008 004, 2008

3. Xiao Q, Tsai HM and Papamoschou D, "Numerical investigation of supersonic nozzle flow separation", AIAA Journal, 45(3), 532-541, 2007

4. P.Reijasse, B.Corbel and D.Soulevant, "Unsteadiness and Asymmetry of shock-Induced Separation in a planar two- Dimensional Nozzle: A Flow Description", Paper AIAA 1999-3694, 1999

5. Papamoschou D and Zill A, "Fundamental investigation of supersonic nozzle flow separation", Paper AIAA 2004-1111, 2004

6. Hunter, C.A., "Experimental, Theoretical and Computational Investigation of Separated Nozzle Flows" Paper AIAA,1998-3107, 1998

ISBN : 978-81-921580-8-2

7. Craig A. Hunter, "Experimental Investigation of Separated Nozzle Flows", AIAA Journal 20(3),527-532, 2004

8. G. Hagemann, M.Frey and W.Koschel, "Appearance of Restricted Shock Separation in Rocket Nozzle", Journal of Propulsion and Power, 18(3), 577-584, 2002

9. A.Gross and C.Weiland, "Numerical Simulation of Separated Cold Gas Nozzle Flows", Journal of Propulsion and Power, 20(3), 509-519, 2004

10. Jan Ostlund, Tomas Damgaard and Manuel Frey, "Side-Load Phenomena in Highly Overexpanded Rocket Nozzles", Journal of Propulsion and Power, 20(4), 695-704, 2004

11. J. Ostlund and B. Muhammad-Klingmann, "Supersonic Flow Separation with Application to Rocket Engine Nozzles", Applied Mechanics Review, Vol. 58, 143-176, 2005

12. Chen C. L., Chakarvarty S. L. and Hung C. M., "Numerical investigation of separated Nozzle Flows", AIAA Journal Vol.32, 1836-1843,1994

13. Nasuti F. and Onofri M., " Viscous and Inviscid vortex generation during startup of Rocket Nozzles", AIAA Journal 36(5), 809-815,1998

14. K. C. Muck, Jean-Paul Dussauge and S. M. Bogdonoff, "Structure of the Wall Pressure Fluctuations in a Shock-Induced Separated Turbulent Flow", Paper AIAA 1985-0179, 1985

15. W. J. Baars, C. E. Tinney, J. H. Ruf, A. M. Brown and D.M. McDaniels, " On the Unsteadiness associated with Shock-Induced Separation in Over-expanded Rocket Nozzles", 46th AIAA/ASME/SAE/ASEE Joint Propulsion Conference and Exhibit, 2010-6728, 2010

16. Zill A, "Flow separation in rectangular over-expanded supersonic nozzles", Paper AIAA 2006-17, 2006

ISBN : 978-81-921580-8-2